Accuracy Benchmark of Galileo and EGNOS for Inland Waterways

Gökay Yayla[a*], Senne Van Baelen[a], Gerben Peeters[a], Muhammad Raheel Afzal[a], Tim Catoor[a], Yogang Singh[a], Peter Slaets[a]

[a]*Intelligent Mobile Platforms (IMP) Research Group, Department of Mechanical Engineering, KU Leuven, Belgium*

[*]Corresponding author. Email: gokay.yayla@kuleuven.be

Synopsis

While Global Navigation Satellite Systems (GNSS) serve as a fundamental positioning technology for autonomous ships in Inland Waterways (IWW), in order to compensate for unexpected signal outages from constellations due to structures such as bridges and high buildings, it is not uncommon to use a sensor fusion setup with GNSS and Inertial Measurement Units (IMU)/Inertial Navigation Systems (INS). However, the accuracy of this fusion relies on the accuracy of the main localization technology itself. In Europe, Galileo and the European Geostationary Navigation Overlay Service (EGNOS) are two satellite navigation systems under civil control and they provide European users with independent access to a reliable positioning satellite signal, claiming better accuracy than what is offered by other accessible systems. Therefore, considering the potential utilization of these systems for autonomous navigation, in this paper, we discuss the results of a case study for benchmarking the accuracy of Galileo and EGNOS in IWW. We used a Coordinate Measurement Machine (CMM) and a sub-cm Real-Time Kinematic (RTK) service which is available in Flanders to quantify the benchmark reference. The results with and without sensor fusion show that Galileo has a better horizontal accuracy profile than standalone Global Positioning System (GPS), and its augmentation with EGNOS is likely to provide European IWW users more accurate positioning levels in the future.

Keywords: Positioning accuracy; GNSS; Galileo; EGNOS; Inland Waterways

1 Introduction

Galileo is Europe's Global Navigation Satellite System (EGNSS) and EGNOS is Europe's regional satellite-based augmentation system (SBAS). As a part of the Horizon 2020 program, a consortium of European research institutes has begun work on the Hull-to-Hull (H2H) project that focuses on a positioning engine utilizing Galileo and EGNOS (H2H, 2020). This system will allow vessels to sail in close proximity to each other by displaying the 2D/3D geometry of the vessel's hull or the object on an electronic chart with an uncertainty zone representing the localization accuracy (Kotzé et al., 2019).

KU Leuven is responsible for the IWW implementation of the H2H system. As signal outages are common in IWW, GNSS systems need to be supported with additional navigation sensors. In this study, an IMU/INS is chosen because it allows dead reckoning navigation during signal outages by computing the position, velocity, and attitude. Furthermore, vulnerabilities and error characteristics of inertial sensors and GNSS receivers are complementary (Demoz, 2009), making them an ideal sensor fusion solution for IWW. However, the accuracy of the positioning technology has a dramatic effect on the accuracy of this fusion. Moreover, inland vessels have spatial limitations leading to more precise localization requirements. Therefore, the purpose of this study is to present a comparative analysis of the positioning accuracies of (i) a standalone GNSS sensor and (ii) loosely coupled GNSS/IMU sensors using GPS, Galileo, and EGNOS on the same trajectory, considering the potential utilization of the H2H system for autonomous navigation in Europe IWW in the future. As most accuracy analysis examples available in the literature (González et al., 2015; Munguia, 2014) usually focus on positioning with GPS and using a low-grade IMU, this paper aims to address the gap in comparative analysis with Galileo, EGNOS, and RTK positioning using a high-end multi-constellation GNSS receiver and a tactical grade IMU/INS system. We conducted our experiments at the Leuven-Dijle Canal on a 1/8 scale model of a CEMT-I (De Conférence Européenne des Ministres de Transport) vessel class (Peeters et al., 2019, 2020), shown in Figure 1. To obtain correct navigation data with GNSS/IMU fusion, we performed an accurate calibration of these onboard sensors.

This paper continues as follows, section 2 introduces the sensors used, section 3 defines the ground truth and our approach to validate its accuracy (sub-cm) with a better static comparison reference (sub-mm), section 4 explains the calibration procedure, section 5 benchmarks the localization results with different positioning modes, and lastly section 6 discusses our findings.

Authors' Biographies

Gökay Yayla, **Senne Van Baelen** and **Tim Catoor** are research staff at the IMP group and working on autonomous inland shipping projects.
Gerben Peeters is a doctoral student at the IMP group and working in the area of autonomous inland shipping.
Dr Muhammad Raheel Afzal is currently a postdoctoral researcher. He manages research and collaboration activities of the IMP group.
Dr Yogang Singh is currently a postdoctoral researcher at the IMP group and working on control strategies for inland waterway vessels.
Prof. Peter Slaets is the head of the IMP group and main coordinator of all the projects under the IMP group.

 https://doi.org/10.24868/issn.2631-8741.2020.009

Figure 1: Scale Model Barge (Cogge).

2 Equipment Installation

The sensors we used in our tests are a Septentrio AsteRx-U Marine GNSS receiver with two PolaNt* MC antennas and an SBG Ekinox-2E IMU/INS. All these components are rigidly fixed to the vessel body frame. In this dual antenna setup, the main (aft) antenna is used for the GNSS position of the vessel and the auxiliary (fore) antenna is used to calculate the orientation using pitch and yaw angles. Therefore both antennas are installed on the centerline of the boat and at the same height from the boat top plate (Figure 2). Additionally, another

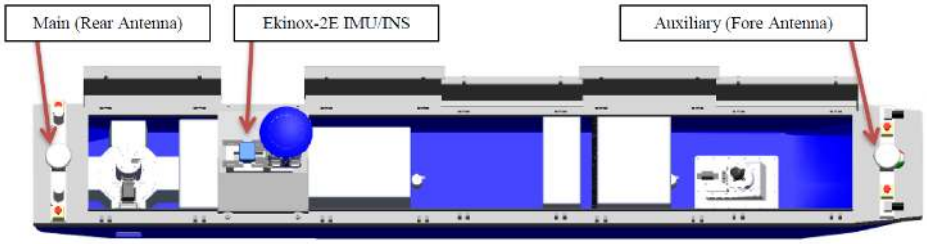

Figure 2: Positions of the sensors on the body frame.

identical GNSS receiver (GNSS-2) is installed next to the other receiver (GNSS-1). This enabled us to log the localization data to be benchmarked from one receiver and the ground truth data from the other receiver on the same trajectory. Signals from both antennas are split 10 cm before the receivers to feed them with the same signals without significant loss.

The INS of Ekinox-2E runs a real-time loosely coupled Extended Kalman Filter (EKF) as the standard method. In this fusion, the INS and GNSS receivers operate as independent navigation systems and the data from them is blended using an estimator to form a third navigation solution (Demoz, 2009). The internal EKF predicts states at 200Hz, based on the integration of its gyroscopes and accelerometers, and these states get a corrective step at 5Hz provided by the GNSS receiver. Figure 3 shows how IMU and external sensors are used inside the EKF to provide navigation and orientation data.

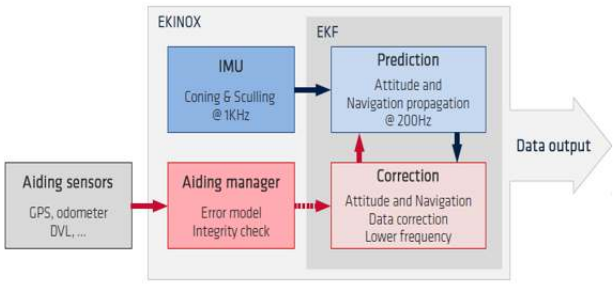

Figure 3: Working principle of the INS (SBG, 2018)

 https://doi.org/10.24868/issn.2631-8741.2020.009

3 Quantification of the Benchmark Reference Results

3.1 Coordinate Frames

This paper uses two coordinate frames (Figure 4). The navigation frame is a fixed frame whose axes point in the north, east, and down directions with a local geodetic origin with the coordinates $50.901654°N - 004.707101°E$ and $16m$ above the mean sea level. The navigation frame will be identified with n. The body frame, identified with b, is a moving frame formed by the axes of the main antenna which are assumed to align with the front, right and down directions of the motions of the vessel being positioned. As the dual-antenna setup is our reference sensor for orientation, the auxiliary antenna is assumed to be on the x-axis of the body frame. Additionally, the top plate of the vessel is assumed to be aligned with the y-axis.

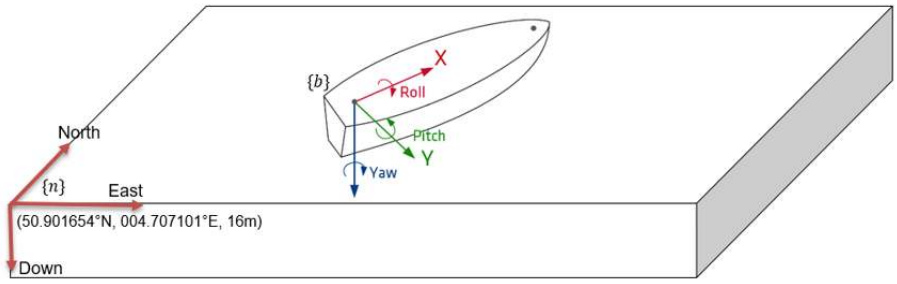

Figure 4: Coordinate frames and the positive directions in the body frame.

3.2 CMM Measurements

Ground truth reference for the relative positions of the onboard sensors is obtained with a Nikon K600 CMM which has up to $90\mu m$ accuracy. Measurements were taken indoors in the Robotics Lab of KU Leuven Mechanical Engineering Department using the sensor reference points shown in Figure 5.

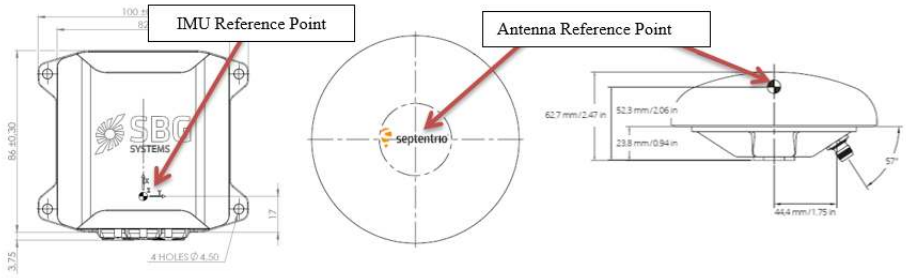

Figure 5: Reference points of the sensors (SBG, 2018; Septentrio, 2018)

Table 1 presents the relative positions (lever arms) of the sensors on the body frame. We have also measured the roll, pitch, and yaw angles of the IMU as $-4.04°$, $2.42°$, and $-1.83°$ respectively. Although these values are

Table 1: CMM measurements.

Reference Point	**X** (*mm*)	**Y** (*mm*)	**Z** (*mm*)
Main Antenna	0	0	0
IMU/INS	946.041	1.051	36.181
Auxiliary Antenna	4435.098	0	0

used mainly for validation of the calibration process, the precisely measured fixed distance between two antennas also used to benchmark the accuracy of the RTK-based positioning which will provide the ground truth in our experiments.

 https://doi.org/10.24868/issn.2631-8741.2020.009

3.3 Ground Truth Information

The localization results are benchmarked using a high precision RTK service available in Flanders. As discussed before, an identical GNSS receiver (AsteRx U-Marine) is installed on the vessel which is able to receive the same signals as the other receiver, establishing the ground truth data using RTK corrections. This is achieved by splitting the signals coming from main and auxiliary antennas just before entering the receivers. This enabled us to quantify the benchmark reference results for every experimental trajectory. Flanders currently has 45 base stations installed for RTK corrections, ensuring a dense coverage, and freely provides this service over mobile internet via the Flemish Positioning Service (FLEPOS). It claims to have $0.009m$ horizontal accuracy within $10km$ of the nearest station (FLEPOS, 2020). In order to justify our selection of the RTK-based positioning as our ground truth, we compared the static measurements of the auxiliary antenna position with the CMM measurements. The distance between our nearest station (Bertem) and our test location (Leuven) was $8km$ and we observed similar results as reported by FLEPOS. The horizontal distance of the auxiliary antenna lever arm from the main antenna is supposed to be $4.435m$ and with FLEPOS we observed this value with a mean value of $4.432m$ and a standard deviation of $0.005m$.

4 Calibration Procedure

Calibration of the IMU/INS includes two main metrics: (i) the location of the IMU, and (ii) the orientation of the IMU on the body frame. To get accurate localization results from the INS, the two GNSS antenna lever arms must be measured. These are the signed distances, expressed in the body (vessel) frame, from the IMU reference point to the GNSS antenna phase center. For orientation, each of the IMU axes must point in the same X, Y, Z directions on the vessel coordinate frame (alignment). Before starting our tests, we performed an auto-calibration with our high-end IMU/INS system (Ekinox-2E) and it was able to estimate the lever arms with sub-cm accuracy. While the details of the calibration procedure are beyond the scope of this paper, it is worthwhile to note that the auto-calibration run was performed dynamically with a 1:8 scale model and it may not always be possible to obtain good estimates due to the scale effect (Heller, 2011) and the need for a larger area to perform dynamic maneuvers, which is not always practical in IWW. We validated the accuracy of the calibration results with our Krypton CMM measurements. For this validation, first, we configured the GNSS receiver to use RTK corrections with all available constellations and feed these values to the INS at 5Hz. Second, we ran a kinematic test and logged GNSS and INS (fusion) output at 50Hz. Then, we benchmarked two positions after transforming the GNSS position to the IMU reference point as the INS position is based on this point. As discussed, the offset originating from the antenna lever arms must be taken into account while updating the INS with GNSS information. Because the position information is coming from the main (aft) antenna, this is the lever arm we are interested in for our post-processing calculations. This lever arm vector is denoted as l^b in the body frame and assumed to be constant over time. The GNSS antenna position transformed to the IMU reference point is as follows:

$$p^n_{REF} = p^n_{GNSS} + R^n_b l^b, \tag{1}$$

where p^n_{GNSS} represents the position vector of the GNSS main antenna in the navigation frame, p^n_{REF} represents the position of benchmark reference for INS position in the navigation frame, and R^n_b represents the rotation matrix from the body frame to the navigation frame. However, it is not possible to fully compose this matrix because the GNSS receiver is only able to calculate the pitch and heading (yaw) angles. Since we do not expect high roll angles, and if we consider the relatively small impact of roll on our calculations, it is reasonable to assume that roll is 0 and rotation around x-axis can be ignored. Then we are able to determine R^n_b. The accuracy of this transformation is a function of the accuracy of the lever arm itself and the accuracy of the orientation solution of the GNSS receiver which takes into account the second lever arm for these calculations. Since we have the accurate vectors measured by a CMM, our transformed GNSS positions will be the benchmark reference for the INS solution.

For the data analysis, we first calculated the IMU reference position vector in the navigation frame (p^n_{REF}) for each timestamp (observation) using the above-mentioned formula. Then the position error vector is calculated by using the position data from INS as follows:

$$\varepsilon = p^n_{INS} - p^n_{REF}, \tag{2}$$

where p represents a position vector $\begin{bmatrix} p_{north} \\ p_{east} \end{bmatrix}$, and p^n_{INS} is the position vector from the INS. We exclude altitude measurements because it does not make any significant difference for navigation purposes in IWW. Positioning errors of the INS output in each direction after the calibration are presented in Figure 6.

According to Figure 6, the error profiles in North and East directions seem to be adequately fit to a normal distribution with the following parameters in meters and acceptable:

$$\varepsilon_{north} \sim \mathcal{N}(-0.0001, 0.0097^2)\,,\ \varepsilon_{east} \sim \mathcal{N}(-0.0001, 0.0078^2)\,.$$

 https://doi.org/10.24868/issn.2631-8741.2020.009

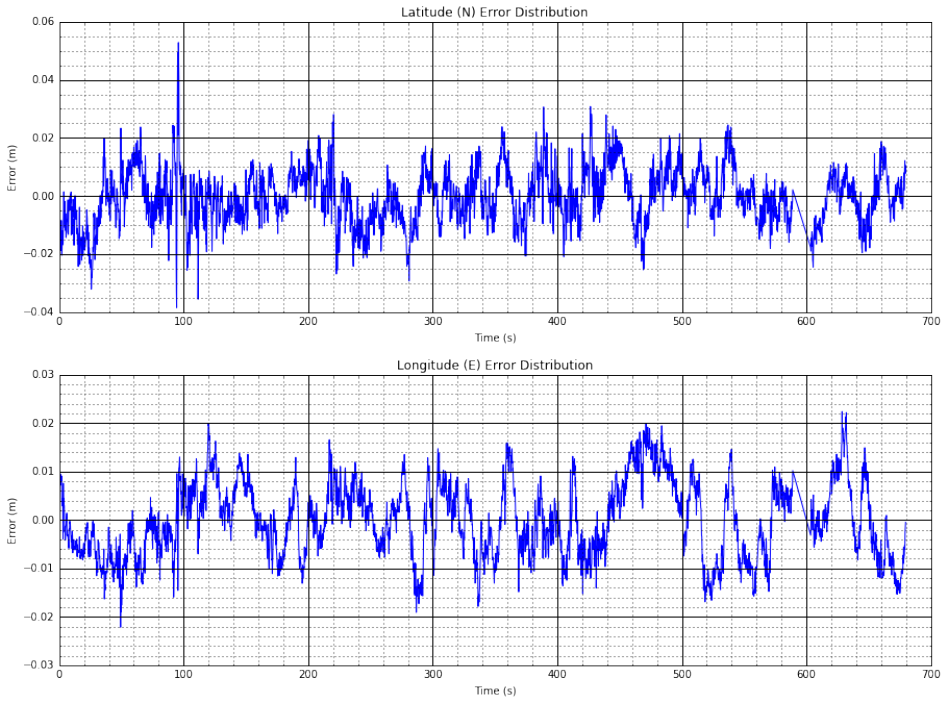

Figure 6: Positioning Errors of the INS.

where $\mathcal{N}(\mu, \sigma^2)$, denotes a normal distribution with a mean of μ and a standard deviation of σ.

Second, the orientation error is calculated as follows:

$$\varepsilon = \psi^n_{INS} - \psi^n_{REF}, \tag{3}$$

where ψ^n_{INS} and ψ^n_{REF} represent the heading angles calculated by the INS and the GNSS receiver respectively. Figure 7 presents the heading error from the INS. Here, we again exclude the roll and pitch as they are not essential for the purpose of this study.

Figure 7: Orientation Error of the INS.

According to Figure 7, there is a clear bias in the heading orientation error ($\mathcal{N}(-1.724°, 0.124^2)$) which is in line with the yaw misalignment we measured with the Krypton CMM (1.83°). In order to remove this misalignment, Ekinox-2E IMU/INS allows for a correction by entering the misalignment angle and running a fine calibration run. After this step, the errors were within the acceptable limits (below $0.01m$ on X and Y axis, and below $0.1°$ on heading angle) for the next step of our experiments.

5 Benchmarking

This section benchmarks the GNSS and INS outputs in different positioning modes with the ground truth reference trajectory obtained using RTK corrections with FLEPOS. We will present the error distributions to investigate any bias and also compare the horizontal Root Mean Square Error (RMSE) as 2 times the RMSE (2RMSE) is the most commonly used accuracy metric in GNSS accuracy reports (FAA, 2017; GSA, 2018), meaning the distance between the true and computed parameter is lower than the stated accuracy with at least a 95% probability.

 https://doi.org/10.24868/issn.2631-8741.2020.009

For benchmarking we performed runs using different positioning methods on the same trajectory at the Vaart/Leuven and logged both the benchmark data (from GNSS-1 and INS) and ground truth data (from GNSS-2) at the same time. Figure 8 presents the common trajectory and speed profiles of the runs.

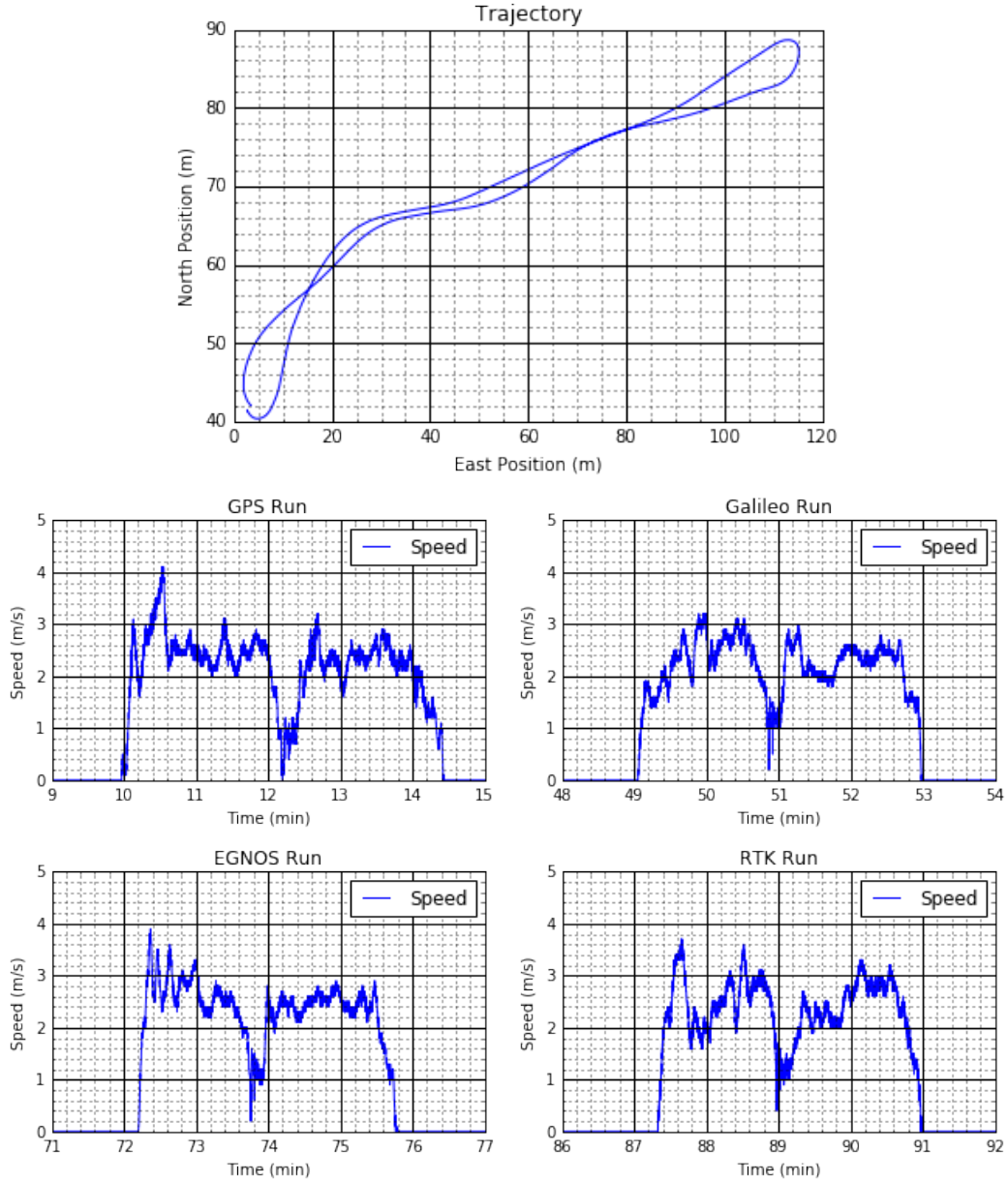

Figure 8: Common trajectory and the speed profiles of the runs.

Before we discuss the INS results, we want to present the raw accuracy of the standalone localization results with GPS, Galileo, and EGNOS that we obtained via our Septentrio AsteRx-U Marine GNSS receiver without fusing the IMU data.

5.1 Standalone localization accuracy of GPS, Galileo, and EGNOS

For this analysis, we will benchmark GNSS-1 data with GNSS-2 data on the same trajectory for each constellation.

GPS:

According to our test results presented in Figure 9, localization using standalone GPS constellation yields error distributions with the following parameters in meters:

$$\varepsilon_{north} \sim \mathcal{N}(0.8221, 0.6474^2)\,,\ \varepsilon_{east} \sim \mathcal{N}(0.3880, 0.2230^2)\,,\ \varepsilon_{down} \sim \mathcal{N}(-2.534, 0.5149^2)\,.$$

The number of satellites used by the GNSS receiver for computing the position was between 9-10.

 https://doi.org/10.24868/issn.2631-8741.2020.009

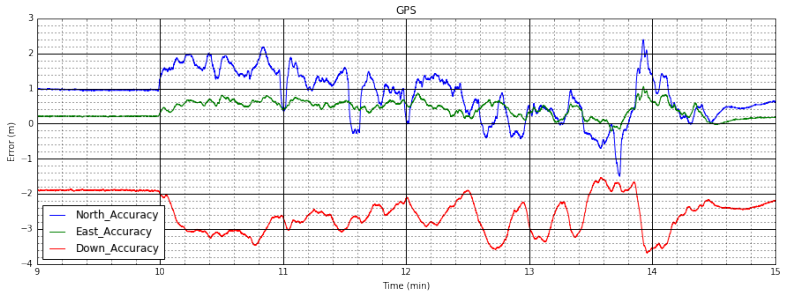

Figure 9: Standalone GPS Accuracy.

Galileo:
According to our test results presented in Figure 10, localization using standalone Galileo constellation yields error distributions with the following parameters in meters:

$$\varepsilon_{north} \sim \mathcal{N}(0.3768, 0.2663^2)\,,\ \varepsilon_{east} \sim \mathcal{N}(0.3367, 0.3124^2)\,,\ \varepsilon_{down} \sim \mathcal{N}(0.5175, 0.1734^2)\,.$$

The number of satellites used by the GNSS receiver for computing the position was between 7-8.

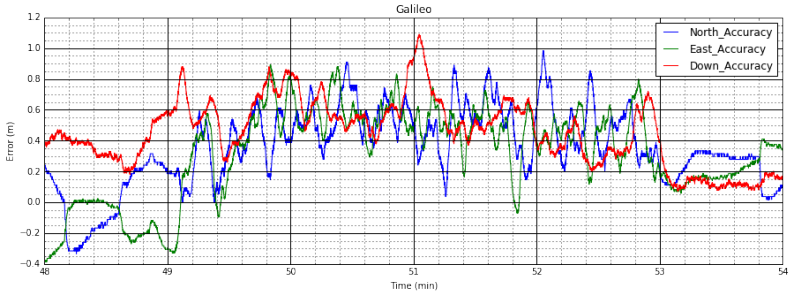

Figure 10: Standalone Galileo Accuracy.

EGNOS:
According to our test results presented in Figure 11, localization using EGNOS as SBAS to GPS constellation yields error distributions with the following parameters in meters:

$$\varepsilon_{north} \sim \mathcal{N}(0.7702, 0.1170^2)\,,\ \varepsilon_{east} \sim \mathcal{N}(0.5997, 0.1148^2)\,,\ \varepsilon_{down} \sim \mathcal{N}(-0.3565, 0.2533^2)\,.$$

The number of satellites used by the GNSS receiver for computing the position was between 8-9.

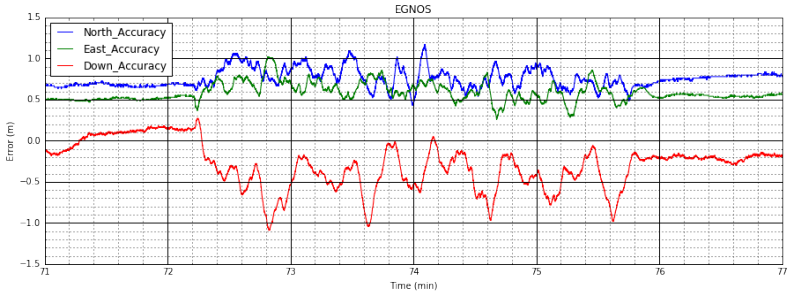

Figure 11: Standalone EGNOS Accuracy.

As shown in the graphs, standalone Galileo and EGNOS have better accuracy performances than standalone GPS. During our experiments, all constellations showed a clear bias to the North and East directions in our test area. But in terms of volatility EGNOS performed the best. We observed that GPS had a very stable static error profile, but when the vessel started moving, volatility increased, especially in the North direction. With Galileo, on the other hand, we observed that the dynamic errors were more than twice as static errors. EGNOS showed a similar error profile as GPS but decreased the mean error and volatility of GPS dramatically (around 0.5m in the

 https://doi.org/10.24868/issn.2631-8741.2020.009

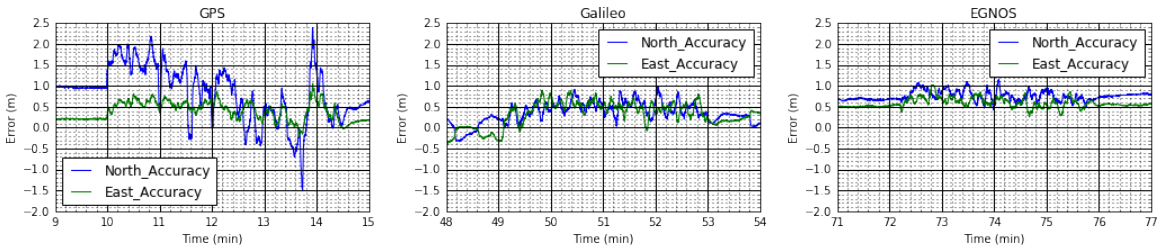

Figure 12: Error Profiles of GPS, Galileo (EGNSS), and EGNOS.

North direction). Considering that the errors in the Down axis are not critical to us, we can compare the results in the North and East directions visually in Figure 12.

While figures above compare the errors on each axis, Table 2 below presents the static and dynamic RMSE metrics of the constellations for the horizontal distance error, which is the Euclidean distance between the observed position and the ground truth.

Table 2: Horizontal Distance Error of Each Constellation.

	Static		Dynamic		
Constellation	**RMSE**	**2RMSE**	**RMSE**	**2RMSE**	**Used Satellites**
GPS	0.694m	1.388m	0.824m	1.648m	9-10
Galileo (EGNSS)	0.198m	0.396m	0.460m	0.920m	7-8
SBAS (EGNOS)	0.594m	1.188m	0.699m	1.398m	8-9

5.2 Benchmarking of the INS results

This section will benchmark the observed data from the INS receiving corrections from different GNSS modes against the ground truth. Our tests are designed as four correction scenarios: (1) Standalone GPS, (2) Standalone Galileo, (3) EGNOS, and (4) RTK. As shown in Figure 8 we performed our tests on the same trajectory at the Vaart/Leuven. Figure 13 and 14 presents the error profiles of the INS localization and orientation results for each scenario.

Table 3 summarizes the error distributions and corresponding static and dynamic RMSE values of each case along with the number of satellites used by the GNSS receiver for computing the position. During the experiments, the number of satellites used for computing the ground truth data varied between 13 and 17.

Table 3: Benchmarking of H2H Sensor Module localization results.

	Horizontal Accuracy		**Latitude**		**Longitude**		**Heading**		**Satellite**	
	Static	**Dynamic**	**(N) (m)**		**(E) (m)**		**(°)**		**Number**	
	2RMSE (m)	2RMSE (m)	μ	σ	μ	σ	μ	σ	min	max
GPS	1.439	1.688	0.838	0.690	0.329	0.379	-0.053	0.116	9	10
Galileo (EGNSS)	0.558	1.014	0.352	0.306	0.392	0.380	0.010	0.104	7	8
SBAS (EGNOS)	1.212	1.398	0.751	0.177	0.597	0.133	-0.020	0.105	8	9
RTK (FLEPOS)	0.018	0.029	0.006	0.029	-0.001	0.028	-0.046	0.107	8	10

The results show that the INS results have similar error profiles as one can expect from the GNSS receiver without sensor fusion. Note that, we had better accuracy with RTK during our calibration benchmarking (Figure 6). However, the slight error increase here originates from a couple of outliers that can be observed in Figure 13. If they are excluded, the accuracy would converge close to zero again. The bottom line is that an INS with RTK corrections yields the best localization performance for IWW navigation. In case of RTK unavailability, Galileo and EGNOS could be the preferred backup modes. While Galileo has a better RMSE, considering the bias in

 https://doi.org/10.24868/issn.2631-8741.2020.009

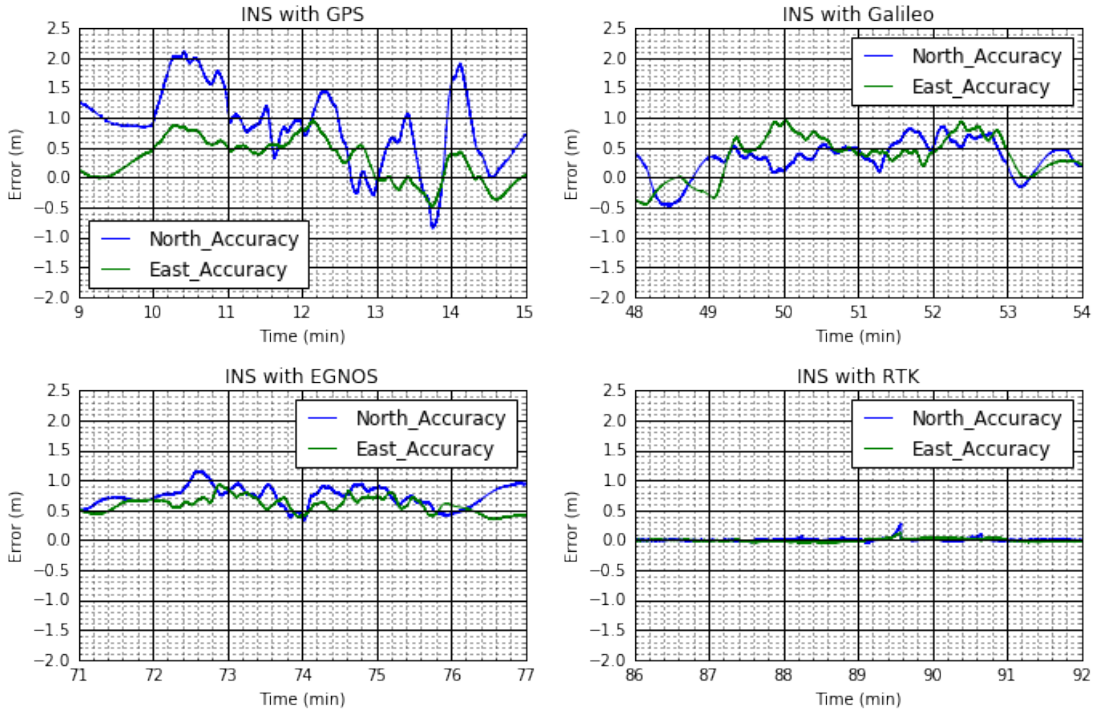

Figure 13: INS localization performance with different positioning modes.

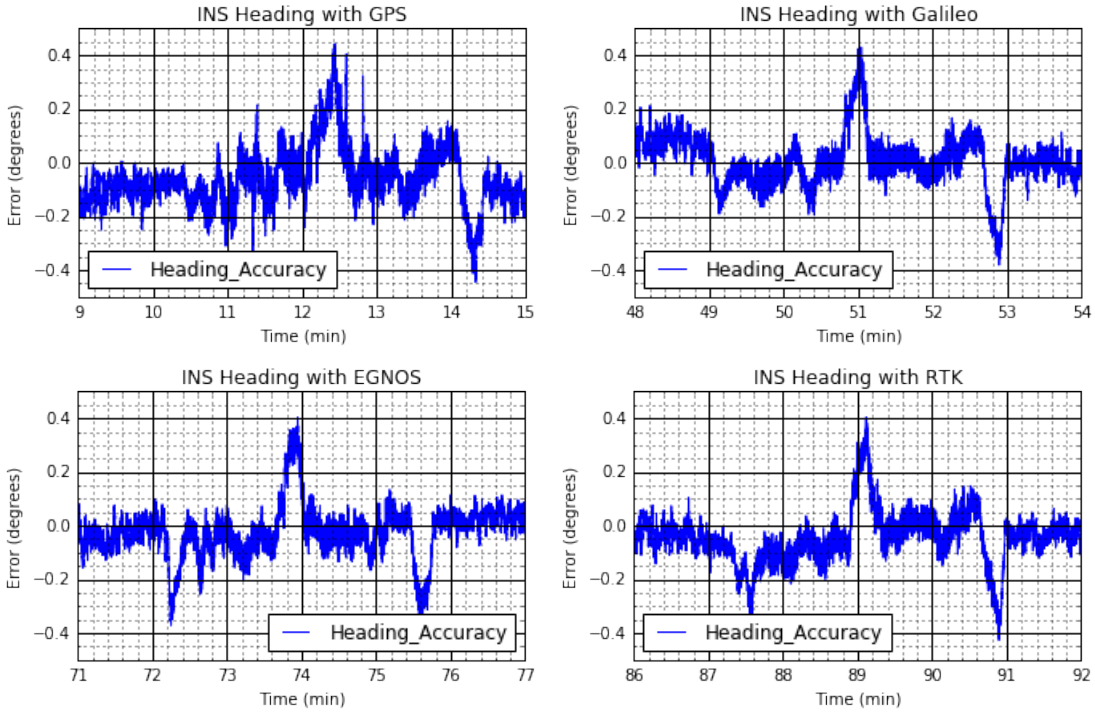

Figure 14: INS orientation performance with different positioning modes.

North and East directions, EGNOS has lower variation. Depending on the satellite coverage and fix quality of the receiver, EGNOS may outperform Galileo in some areas or under certain conditions. Therefore, in order to decide between both options, more experiments can be done depending on the operating area of the vessel. But, it can also be advised to prefer EGNOS to Galileo for auto-calibration purposes where low volatility is desired.

 https://doi.org/10.24868/issn.2631-8741.2020.009

6 Conclusion and Discussion

In this paper, we have presented the benchmarking of the positioning results of a loosely coupled IMU/INS system with a GNSS receiver on a scale model vessel in IWW. First, we explained the calibration procedure and discussed its accuracy. Then after removing any systematic errors by performing a fine calibration, we evaluated the accuracy of the localization results from both the standalone GNSS receiver and the INS for different GNSS modes (standalone GPS, standalone Galileo, EGNOS and RTK) in comparison to an accurate reference trajectory. We used a highly accurate (sub-cm) RTK service called FLEPOS to generate the ground truth trajectory for our tests and explained the validation with a sub-mm metrology device (Krypton CMM). Results showed that standalone Galileo and EGNOS have lower errors than standalone GPS. Afterwards, we benchmarked the results of the INS for 4 different GNSS correction modes. While for the RTK case, the accuracy is very high as expected, with other cases, the INS suffers from errors of up to 2m in Latitude and 1m in Longitude accuracy. However, our experiments show that the accuracies are slightly better than publicly announced horizontal accuracies (2RMSE) of GPS and Galileo, which are 1.9m for GPS (FAA, 2017) and 1.5m for Galileo (GSA, 2018). For EGNOS, we observed 0.1m worse performance than the accuracy value declared in the latest report (ESSP, 2020), which is 1.3m. However, EGNOS provided better stability with a lower volatility compared to other constellations. In case of RTK unavailability, one can choose from Galileo or EGNOS options as the main positioning mode. According to the results, although Galileo is a better choice in terms of horizontal accuracy, our experiments show that because of its low volatility EGNOS could also be an alternative depending on the accuracy requirements of the user. Our results in section 5 support this argument by showing the improvement both in terms of accuracy and volatility. Given that EGNOS will also be compatible with Galileo in the future, it is likely that European users will reach more accurate positioning levels with EGNOS. Lastly, vessels in IWW usually sail at the same area or routes and this benchmarking could be a reasonable approach especially for this type of vessels to understand if there is an expected positioning bias in each axis under certain conditions and investigate ways to eliminate them.

Acknowledgement

This work is supported by the European GNSS Agency (GSA) under the grant agreement No 775998 associated with the project "EGNSS Hull to Hull (H2H)" (H2H, 2020).

References

The Hull-to-Hull (H2H) Project, 2020. URL: https://www.sintef.no/projectweb/hull-to-hull/.

Kotzé M., Junaid A.B, Afzal M.R., Peeters G., Slaets P., 2019. Use of Uncertainty Zones for Vessel Operation in Inland Waterways. J. Phys. Conf. Ser.

Demoz G., Gleason S., 2009. GNSS Applications and Methods. Artech House.

González R., Giribet J.I, Patiño H.D., 2015. An approach to benchmarking of loosely coupled low-cost navigation systems. Mathematical and Computer Modelling of Dynamical Systems, URL: https://doi.org/10.1080/13873954.2014.952642.

Munguia R., 2014. A GPS-aided Inertial Navigation System in Direct Configuration. Journal of Applied Reasearch and Technology, 803-814.

Peeters G., Catoor T., Afzal M.R., Kotze M., Geenen P., Van Baelen S., Vanierschot M., Boonen R., Slaets P., 2019. Design and build of a scale model unmanned inland cargo vessel: actuation and control architecture, J. Phys. Conf. Ser.

Peeters G., Kotze M., Afzal M.R., Catoor T., Van Baelen S., Geenen P., Vanierschot M., Boonen R., Slaets P., 2020. An unmanned inland cargo vessel: Design, build, and experiments. IEEE J.Ocean Eng.Vol.201, pp.17, URL: https://doi.org/10.1016/j.oceaneng.2020.107056.

SBG, 2018. Ekinox Surface Series Tactical Grade MEMS Inertial Sensors Hardware Manual. Tech. rep.. SBG Systems.

Septentrio, 2017. AsteRx-U User Manual. Tech. rep.. Septenrio, Leuven.

Flepos, 2020, URL: https://overheid.vlaanderen.be/flepos-algemeen.

Heller, V., 2011. Scale Effects in Physical Hydraulic Engineering Models. Journal of Hydraulic Research, Vol. 49, No. 3, pp. 293–306.

Federal Aviation Administration (USA). GPS Performance Analysis Report, Jan 2017, Available at: https://www.nstb.tc.faa.gov/reports/.

GSA, Galileo Initial Services - Open Service Performance Report, March 2018, Available at: https://www.gsc-europa.eu/.

ESSP, Monthly Performance Report, January 2020, Available at: https://egnos-user-support.essp-sas.eu/.

 https://doi.org/10.24868/issn.2631-8741.2020.009